Understanding Conformational Polymorphism in Ganciclovir: A Holistic Approach

Lorella Spiteri, Ulrich Baisch and Liana Vella-Zarb

SUPPLEMENTARY MATERIAL

A. Intramolecular Geometry

Form I

Type	Fragment	Class	Query value	Std. dev.	| z-score |	Min	Max	Local density
Length	O1 C2	Usual	1.234	0.016	0.192	1.109	1.606	
	O2 C6	Usual	1.421	0.012	1.013	1.388	1.423	
	C3 N3	Usual	1.393	0.013	0.488	1.328	1.489	
	C4 N4	Usual	1.38	0.016	1.307	1.295	1.402	
	C1 N5	Usual	1.325	0.013	0.171	1.233	1.374	
	C1 N1	Usual	1.34	0.014	0.311	1.280	1.399	
	C2 N2	Usual	1.397	0.014	1.086	1.276	1.458	
	C3 C2	Usual	1.423	0.036	0.64	1.376	1.755	
	C4 N3	Usual	1.311	0.021	0.255	1.258	1.566	
	C5 N4	Usual	1.376	0.011	0.481	1.318	1.409	
	C6 N4	Usual	1.441	0.012	1.964	1.437	1.493	
	O2 C7	Usual	1.441	0.014	0.758	1.365	1.465	
	O3 C8	Usual	1.425	0.028	0.183	0.900	1.743	
	O4 C9	Usual	1.435	0.028	0.513	0.900	1.743	
	C1 N2	Usual	1.373	0.014	0.347	1.315	1.425	
	C5 N5	Usual	1.355	0.017	0.683	1.260	1.427	
	C3 C5	Usual	1.382	0.023	0.090	1.302	1.683	
	C8 C7	Usual	1.523	0.02	0.759	1.413	1.578	
	C9 C7	Usual	1.514	0.02	0.292	1.413	1.578	
Angle	C6 O2 C7	Usual	111.837	2.516	0.310	109.984	115.79	
	C1 N2 C2	Usual	126.037	1.261	0.813	119.369	129.626	
	C4 N3 C3	Usual	104.502	1.308	0.012	97.768	108.878	
	C4 N4 C5	Usual	106.591	0.581	1.370	103.748	107.003	
	C6 N4 C4	Usual	126.223	1.877	0.483	123.377	130.018	
	C6 N4 C5	Usual	127.165	1.947	0.205	123.951	130.231	
	C1 N5 C5	Usual	111.95	1.263	0.311	106.601	118.886	

	N1 C1 N5	Usual	120.724	1.057	0.958	114.493	123.191	
	N2 C1 N5	Usual	123.382	0.979	0.177	118.174	127.867	
	N1 C1 N2	Usual	115.883	1.131	0.971	113.019	122.374	
Angle	O1 C2 N2	Usual	120.511	1.394	0.198	110.448	131.372	
	O1 C2 C3	Usual	128.586	2.473	0.811	118.952	135.102	
	C3 C2 N2	Usual	110.864	2.045	0.983	101.087	117.665	
	C2 C3 N3	Usual	130.283	1.667	0.006	125.414	145.667	
	C5 C3 N3	Usual	110.688	0.994	0.166	103.817	114.763	
	C2 C3 C5	Usual	118.884	1.177	0.035	109.771	122.379	
	N4 C4 N3	Usual	112.767	0.911	0.722	110.927	115.918	
	N4 C5 N5	Usual	125.782	1.189	0.065	121.55	128.166	
	C3 C5 N4	Usual	105.452	0.850	0.417	102.939	107.308	
	C3 C5 N5	Usual	128.766	0.911	0.502	125.944	131.565	
	O2 C6 N4	Usual	108.565	3.710	0.358	104.013	112.842	
	O2 C7 C8	Usual	108.521	3.312	0.072	102.620	114.971	
	O2 C7 C9	Usual	107.509	3.312	0.377	102.620	114.971	
	C9 C7 C8	Usual	113.436	2.278	0.153	109.692	119.817	
	O3 C8 C7	Usual	111.385	2.212	0.165	105.684	123.047	
	O4 C9 C7	Usual	110.371	2.212	0.624	105.684	123.047	
Torsion	C7 O2 C6 N4	Usual	173.405					0.067
	O2 C6 N4 C4	Usual	-98.097					0.346
	O2 C6 N4 C5	Usual	83.819					0.406
	C6 O2 C7 C8	Usual	-87.481					0.222
	C6 O2 C7 C9	Usual	149.46					0.278
	O2 C7 C8 O3	Usual	173.901					0.281
	O3 C8 C7 C9	Usual	-66.691					0.406
	O2 C7 C9 O4	Usual	46.573					0.062
	O4 C9 C7 C8	Usual	-73.412					0.312
Ring	N2 C1 N5 C5 C3 C2	Usual				0	6.136	1
	N3 C3 C5 N4 C4	Usual				0	2.907	1

Table A1: Geometric parameters of form I, produced by Mogul. (Organometallic compounds are excluded, R-factor < 7.5%)

Form II

Type	Fragment	Class	Query value	Std. dev.	| z-score |	Min	Max	Local density
Bond	O1 C2	Usual	1.247	0.016	0.988	1.109	1.606	
	O2 C6	Usual	1.423	0.012	1.225	1.388	1.423	
	O3 C8	Unusual	1.334	0.028	3.094	0.9	1.743	
	O4 C9	Usual	1.45	0.028	1.068	0.9	1.743	
	C1 N2	Usual	1.37	0.014	0.088	1.315	1.425	
	C1 N5	Unusual	1.357	0.013	2.328	1.233	1.374	
	C3 N3	Usual	1.375	0.013	0.83	1.328	1.489	
	C5 N4	Usual	1.376	0.011	0.506	1.318	1.409	
	C1 N1	Usual	1.352	0.014	1.133	1.28	1.399	
	C5 N5	Usual	1.352	0.017	0.488	1.26	1.427	
	C3 C5	Usual	1.384	0.023	0.184	1.302	1.683	
	C2 N2	Usual	1.377	0.014	0.351	1.276	1.458	
	C4 N3	Usual	1.309	0.021	0.377	1.258	1.566	
	C6 N4	Usual	1.475	0.012	0.848	1.437	1.493	
	O2 C7	Usual	1.453	0.014	1.578	1.365	1.465	
	C8 C7	Unusual	1.578	0.02	3.48	1.413	1.578	
	C9 C7	Unusual	1.559	0.02	2.529	1.413	1.578	
	C4 N4	Usual	1.364	0.016	0.317	1.295	1.402	
	C3 C2	Usual	1.44	0.036	0.151	1.376	1.755	
Angle	C6 O2 C7	Usual	110.084	2.516	1.006	109.984	115.79	
	C1 N2 C2	Usual	126.93	1.261	1.52	119.369	129.626	
	C1 N5 C5	Usual	111.024	1.263	1.044	106.601	118.886	
	C4 N3 C3	Unusual	100.532	1.308	3.022	97.768	108.878	
	C6 N4 C5	Usual	124.407	1.947	1.212	123.951	130.231	
	C4 N4 C5	Usual	106.067	0.581	0.469	103.748	107.003	
	C6 N4 C4	Usual	129.513	1.877	1.27	123.377	130.018	
	N2 C1 N5	Usual	122.731	0.979	0.487	118.174	127.867	
	N1 C1 N2	Usual	118.303	1.131	1.169	113.019	122.374	
	N1 C1 N5	Usual	118.965	1.057	0.705	114.493	123.191	
	N4 C5 N5	Usual	126.787	1.189	0.911	121.55	128.166	
	C3 C5 N4	Unusual	102.939	0.85	3.373	102.939	107.308	
	C3 C5 N5	Unusual	130.271	0.911	2.154	125.944	131.565	

Type	Fragment	Class	Query value	Std. dev.	| z-score |	Min	Max	Local density
Angle	C5 C3 N3	Unusual	114.498	0.994	3.998	103.817	114.763	
	C2 C3 N3	Usual	128.055	1.667	1.331	125.414	145.667	
	C2 C3 C5	Usual	117.376	1.177	1.316	109.771	122.379	
	O1 C2 N2	Usual	119.51	1.394	0.52	110.448	131.372	
	O1 C2 C3	Usual	128.763	2.473	0.882	118.952	135.102	
	C3 C2 N2	Usual	111.629	2.045	0.609	101.087	117.665	
	N4 C4 N3	Unusual	115.918	0.911	2.737	110.927	115.918	
	O2 C6 N4	Usual	104.298	3.71	0.792	104.013	112.842	
	O2 C7 C8	Usual	108.998	3.312	0.072	102.62	114.971	
	O2 C7 C9	Usual	102.62	3.312	1.853	102.62	114.971	
	C9 C7 C8	Unusual	119.817	2.278	2.954	109.692	119.817	
	O3 C8 C7	Usual	109.406	2.212	1.06	105.684	123.047	
	O4 C9 C7	Usual	107.514	2.212	1.915	105.684	123.047	
Torsion	C7 O2 C6 N4	Usual	152.753					0.067
	O2 C6 N4 C5	Usual	-70.847					0.406
	O2 C6 N4 C4	Usual	110.66					0.423
	C6 O2 C7 C8	Usual	-76.568					0.389
	C6 O2 C7 C9	Usual	155.41					0.389
	O2 C7 C8 O3	Usual	-63.152					0.594
	O3 C8 C7 C9	Usual	54.469					0.594
	O2 C7 C9 O4	Usual	-172.345					0.281
	O4 C9 C7 C8	Usual	66.805					0.406
Ring	N2 C1 N5 C5 C3 C2	Usual				0	5.925	1
	N3 C3 C5 N4 C4	Usual				0	3.177	1

Table A2: Geometric parameters of form II, produced by *Mogul.* (Organometallic compounds are excluded, R-factor < 7.5%) The configuration in form II can be attributed to the relatively high degree of folding present along the ribose chain, which is characterized by several unusually long bond lengths. When taking into account the full molecular structure of form II, it is understandable how the compromise in the orientation could be afforded because of the resultant stability gained through intramolecular coulombic forces.

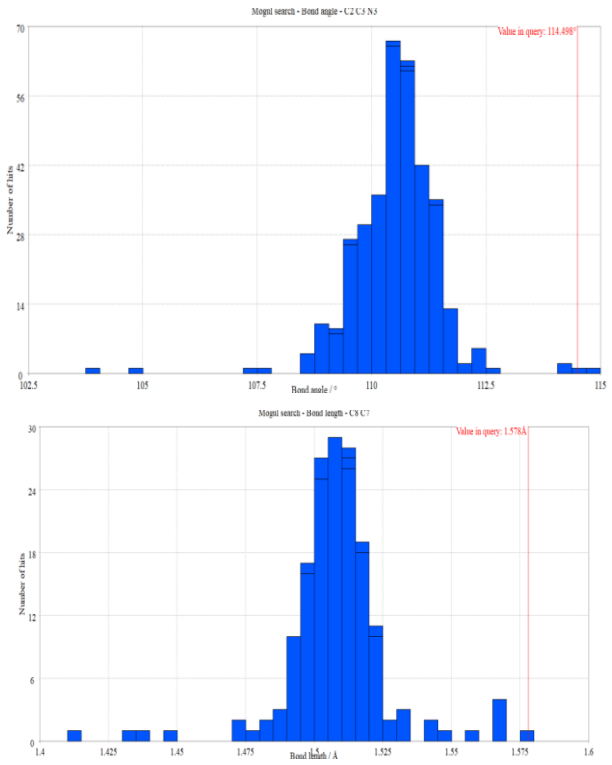

Figure A3: Histogram of the Bond angle C5C3N3 and Bond length C8-C7, together with the query value of form II. All 167 fragments were of maximum relevance to form II fragment, with R-factor ≤ 7.5%.

This suggested that owing to different factors, the molecule of form II compromised its geometric conformation from the usual range of observed parameters, probably due to its high degree of folding.

B: Electrostatic Potential Maps

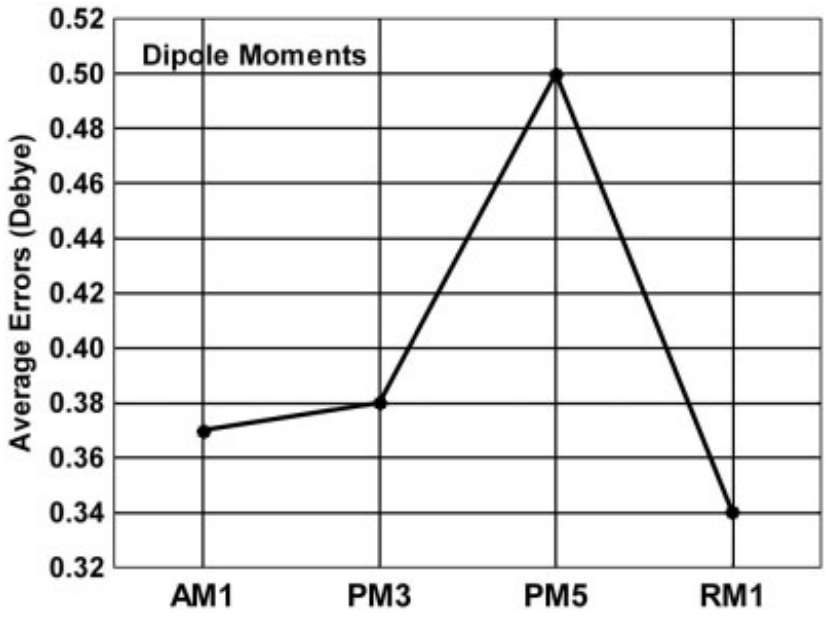

Figure B1: The average errors for dipole moments for 127 molecules, calculated by AM1, PM3, PM5 and RM1.[138]

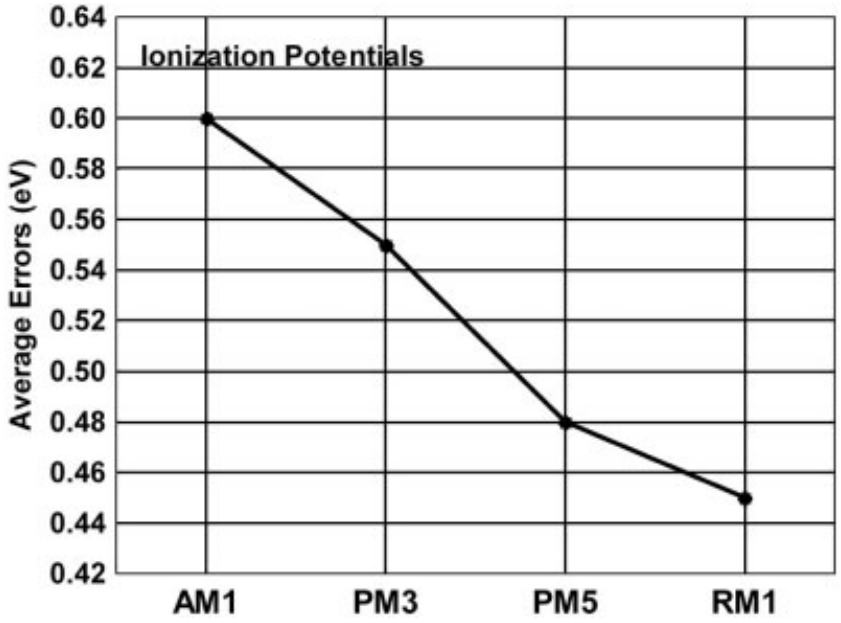

Figure B2: The average errors for ionization potentials for 127 molecules, calculated by AM1, PM3, PM5 and RM1.[138]

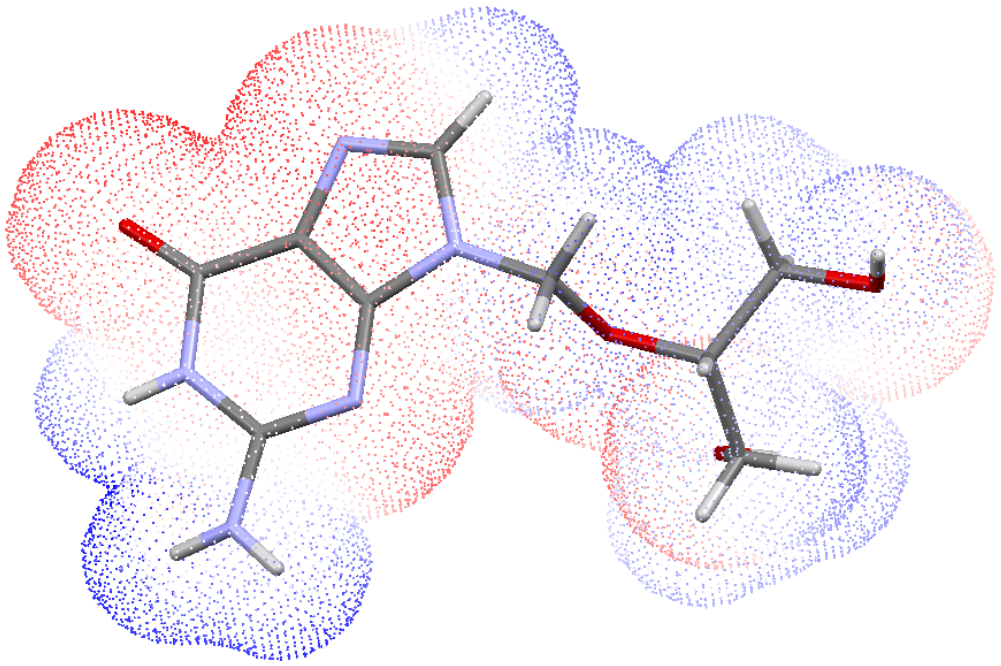

Figure B3: The electrostatic potential map of form II, calculated with RM1 method, through MOPAC interface in *Mercury*.

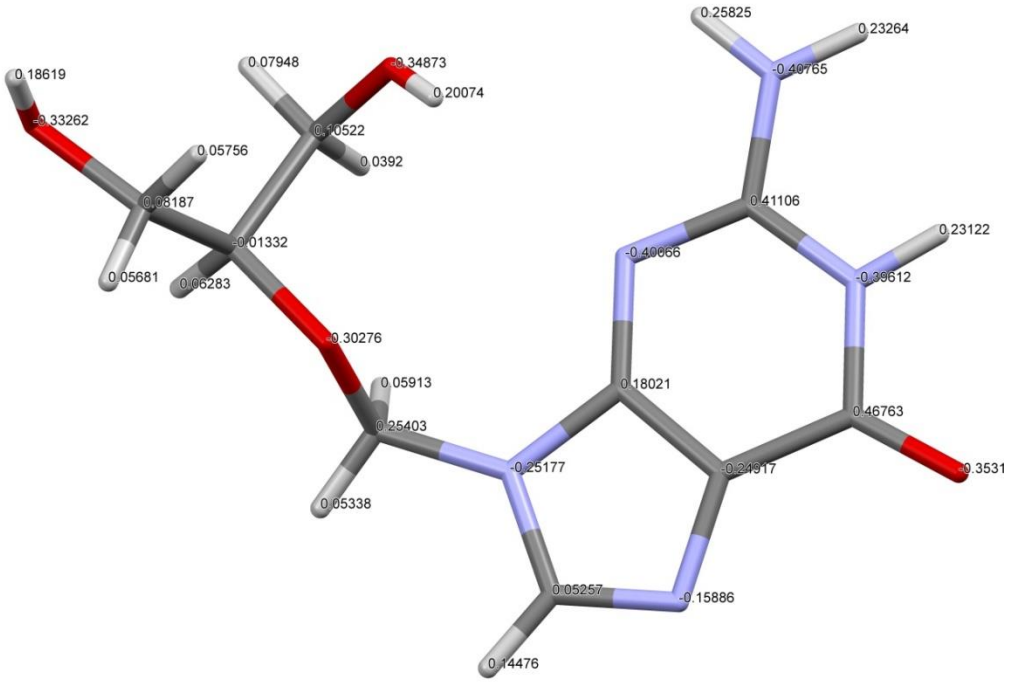

Figure B4: The partial charges of form II, calculated with RM1 method, through MOPAC interface in *Mercury*.

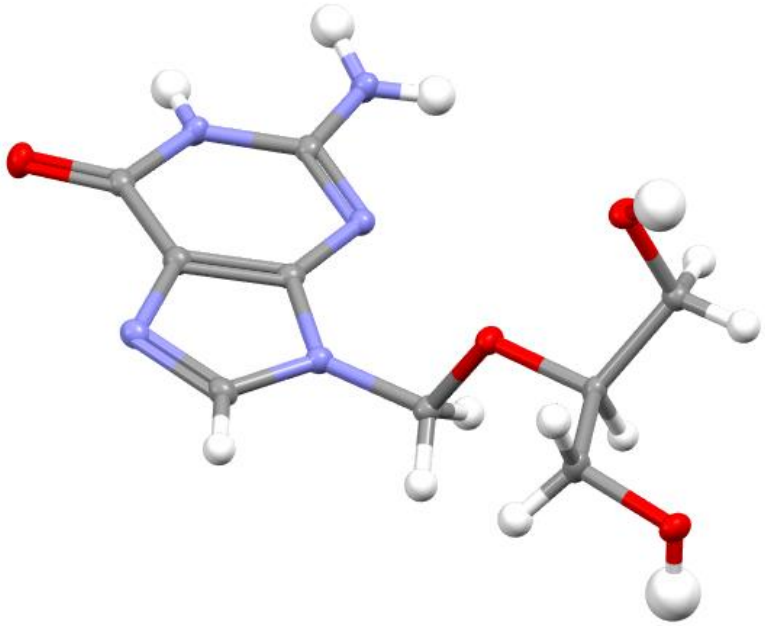

Figure B5: Form I displayed with its displacement ellipsoids, drawn in *Mercury*.

(Probability level = 50%)

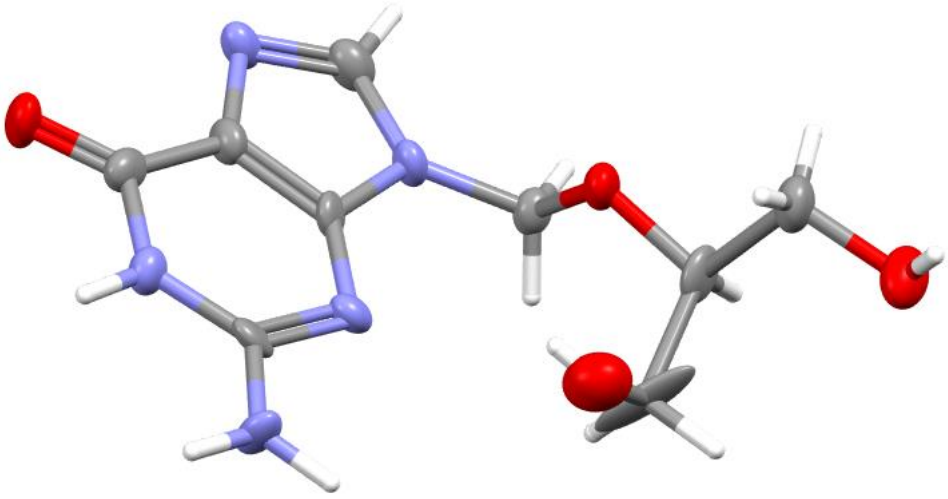

Figure B6: Form II displayed with its displacement ellipsoids, drawn in *Mercury*. (Probability level = 20%)

C. Intermolecular Analysis

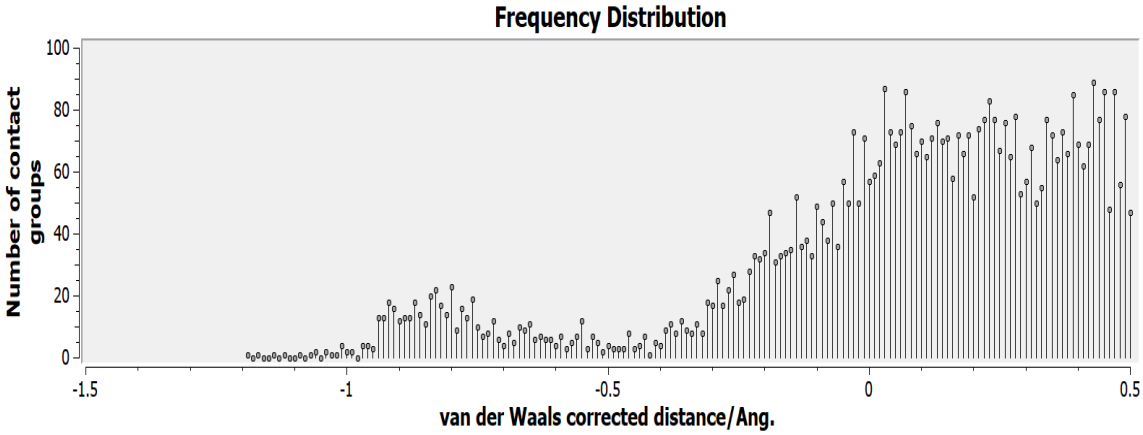

Figure C1: Frequency plot showing the distribution of the number of N-H and O-H groups per corrected distance in Å. Contacts with a length less than the sum of VdW radii have negative values, while those with longer lengths have positive values. This figure shows the dominant presence of contacts with relatively longer intermolecular bond, which are commonly considered as weaker contacts.

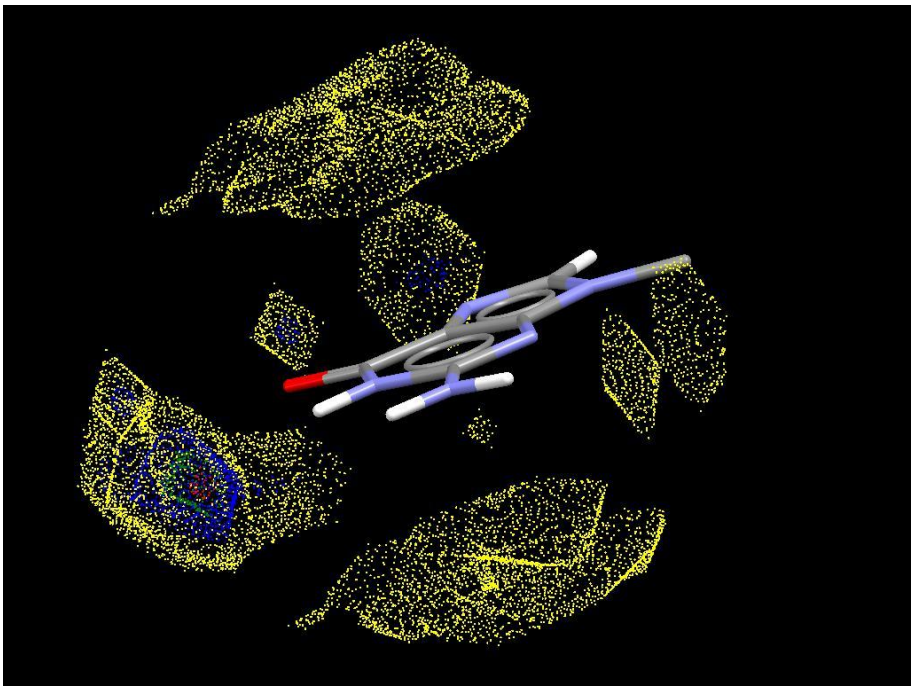

Figure C2: Guanine ring system with only carbon as the contact groups. (Internal scaling: Level 10 – Yellow, Level 25 – Blue, Level 50 – Green, Level 75 – Red)

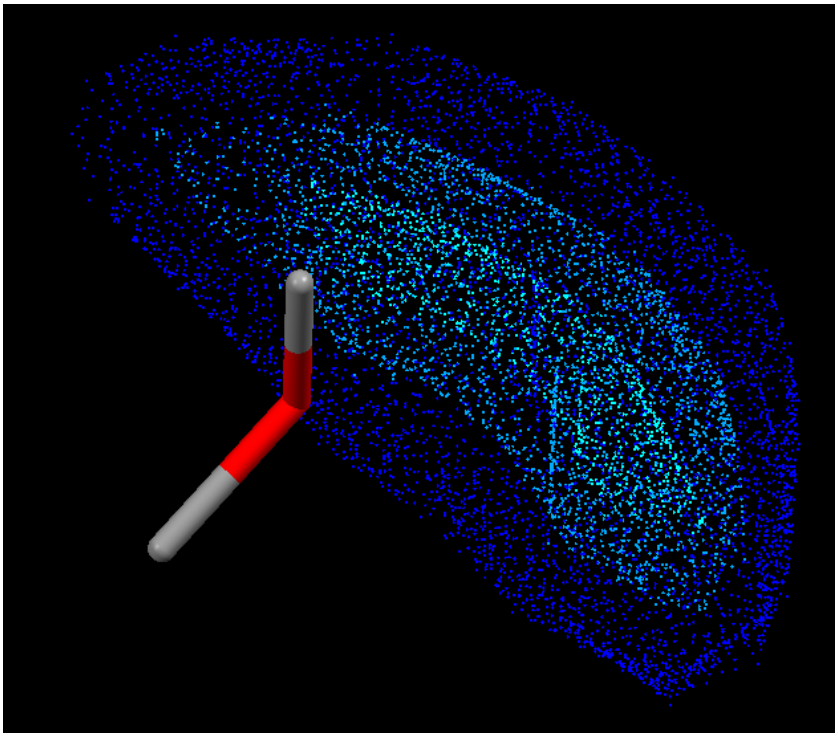

Figure C3: Aliphatic ether as the central group, with nitrogen and oxygen atoms as the contact groups. (Internal scaling: Level 25: Dark Blue, Level 50: Lighter Blue, Level 75: Turquoise)

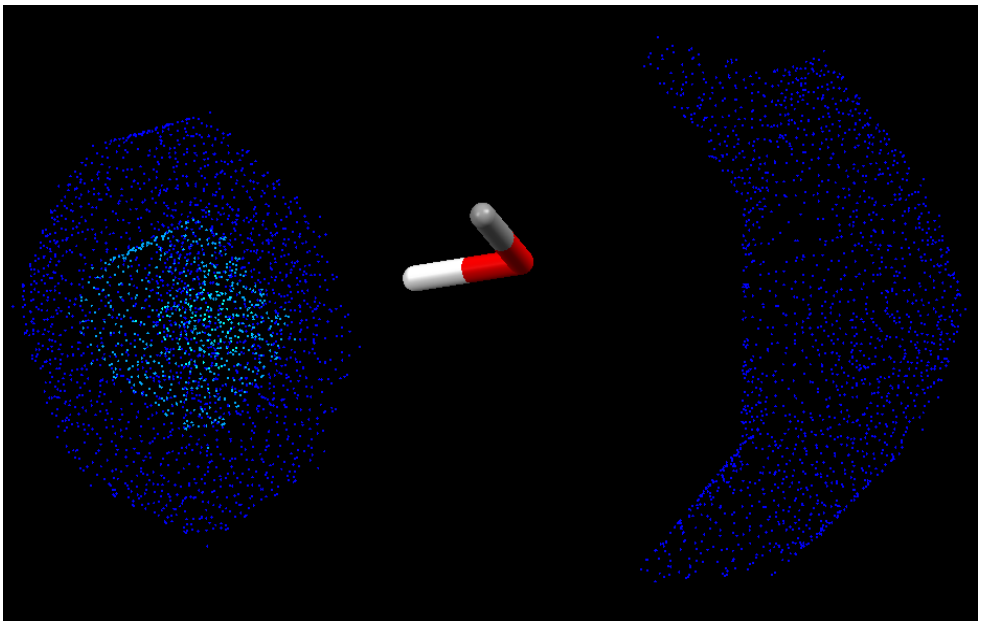

Figure C4: *IsoStar* contour plot of aliphatic hydroxyl group, with nitrogen and oxygen as probes (internal scaling as described in C3).

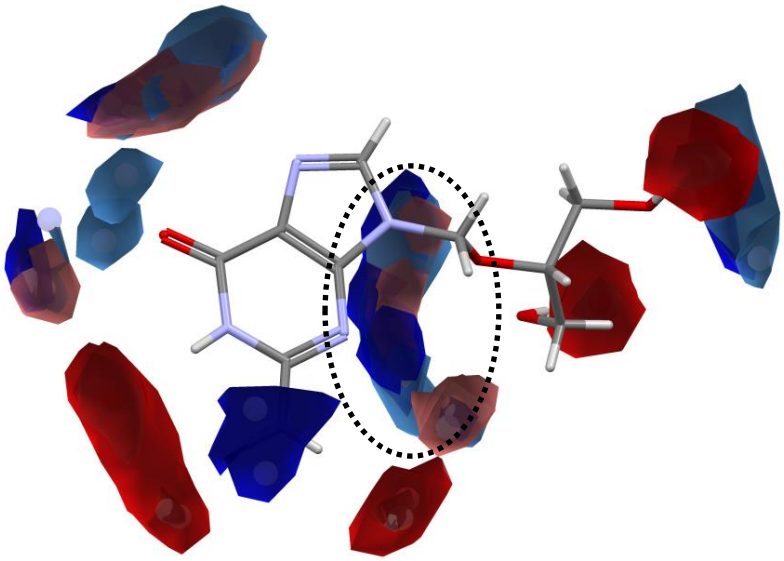

Figure C5: Full interaction map of form I, with uncharged NH nitrogen (blue), RNH3 Nitrogen (light blue), alcohol oxygen (light red) and carbonyl oxygen (red), at level 6.0. The circled area marks the intense interaction map around the ether oxygen.

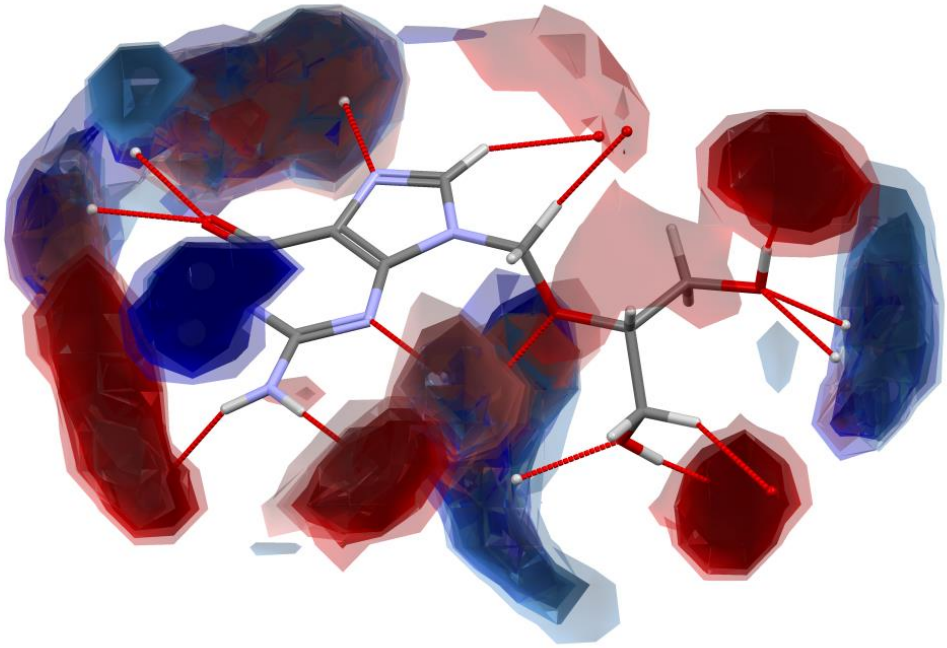

Figure C6: Full interaction map of form I, with uncharged NH nitrogen (blue), RNH3 Nitrogen (light blue), alcohol oxygen (light red) and carbonyl oxygen (red), at levels 2, 4 and 6.

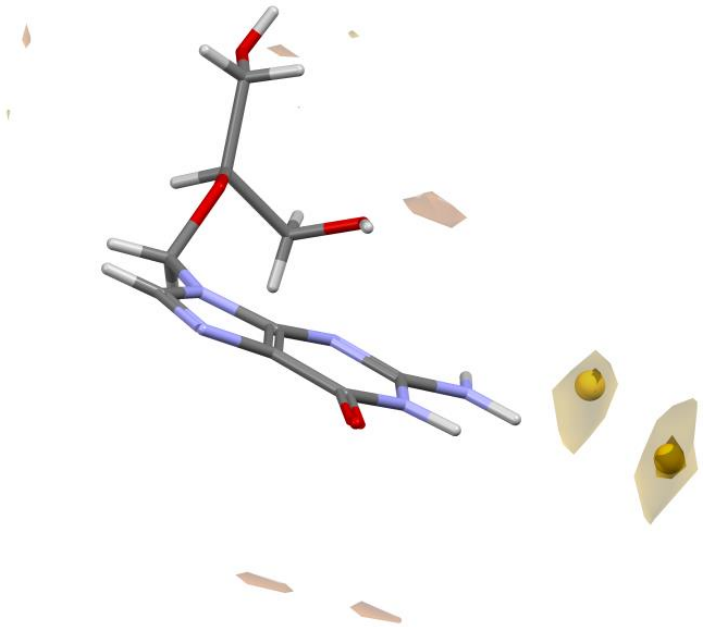

Figure C7: Full interaction map of form II with methyl carbon (yellow) and aromatic C-H (orange) probes, at levels 2, 4 and 6.

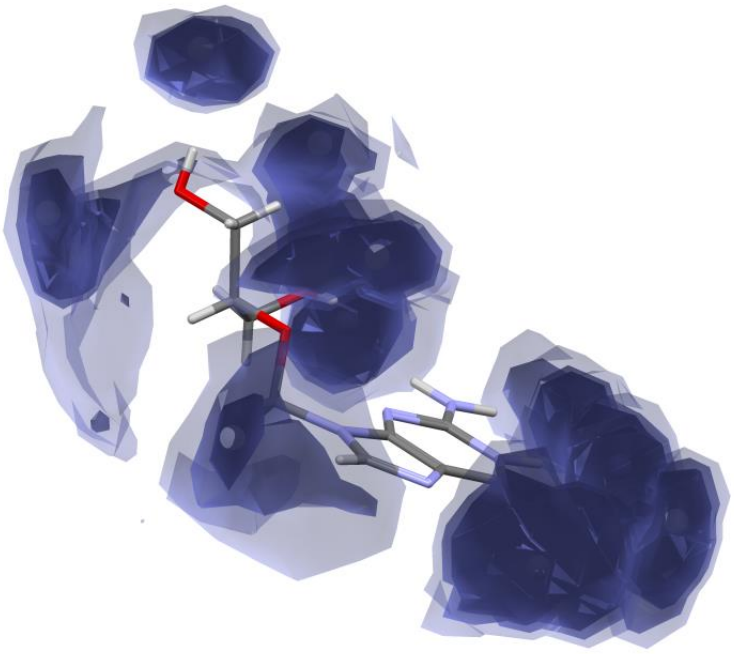

Figure C8: Full interaction Map of form II, with water oxygen as probe at levels 2, 4 and 6.

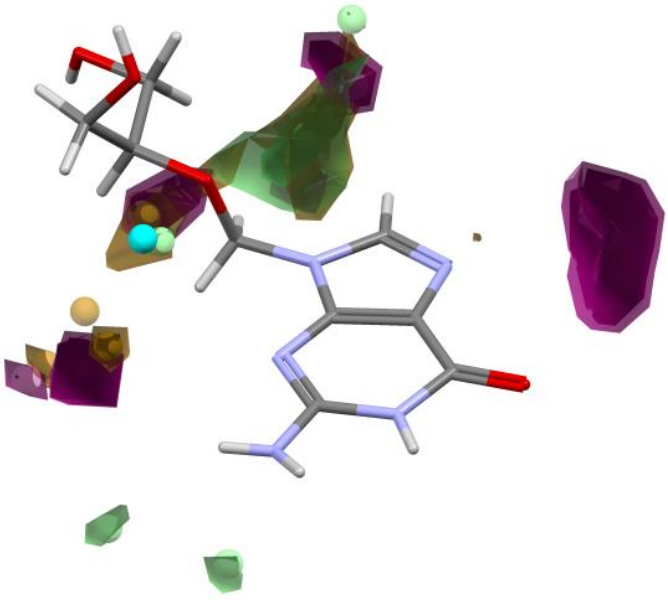

Figure C9: Full interaction map of form I with C-F (turquoise), C-Cl (light green), C-Br (brown) and C-I (violet) as probes, at different levels.

Figure C10: Full interaction map of form II with C-F (turquoise), C-Cl (light green), C-Br (brown) and C-I (violet) as probes, at different levels.

Donor – H ··· Acceptor	Frequency (%)
O3 – H ··· N3	18.0
O4 – H ··· O3	15.4
N1 – H ··· N5	30.9
N2 – H ··· O4	9.09
N1 – H ··· O2	16.9
C4 – H ··· O1	25.5
C6 – H ··· O1	22.2
C9 – H ··· O3	30.2

Table C11: The results of the motif search for the intermolecular contacts in form I.

Donor – H ··· Acceptor	Frequency (%)
N2 – H ··· N3	38.5
N1 – H ··· O1	41.3
N1 – H ··· O4	45.0
O4 – H ··· O1	12.6

Table C12: The results of the motif search for the intermolecular contacts in form II.

Donor – H ··· Acceptor	Contact length (Å)	Contact angle (°)
O3 – H ··· N3	1.923	172.05
O4 – H ··· O3	1.911	175.25
N1 – H ··· N5	2.153	179.37
N2 – H ··· O4	2.072	172.36
N1 – H ··· O2	2.342	142.54
C4 – H ··· O1	2.286	150.76
C6 – H ··· O1	2.467	133.92
C9 – H ··· O3	2.559	136.69

Table C13: Hydrogen bonds present in form I, as defined by PLATON. The numbering corresponds to that present in form I, as illustrated in figure 1a.

Type	Donor – H ··· Acceptor	Contact length (Å)	Contact angle (°)
Intermolecular	N2 – H ··· N3	1.896	166.10
	N1 – H ··· O1	1.924	161.71
	N1 – H ··· O4	2.277	140.56
	O4 – H ··· O1	2.123	150.96
Intramolecular	O3 – H ··· N5	2.549	135.90

Table C14: Hydrogen bonds present in form II, as defined by PLATON. The numbering corresponds to that present in form II, as illustrated in figure 1b. The contacts in form II seem to be more conventional than the ones present in the other anhydrous form, and this observation is also reflected in the frequencies of the motifs search.

D. Supramolecular Analysis

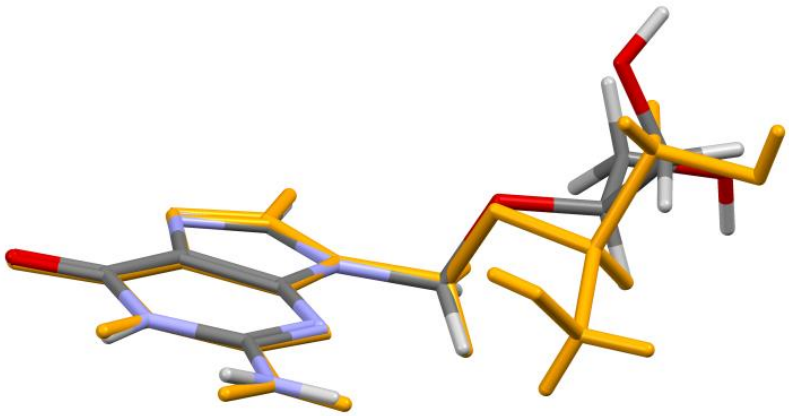

Figure D1: Overlay of structures in order to observe the difference between their configurations. Elemental colours: Form I and Orange structure: Form II. The molecular overlay tool confirmed that the two forms are a result of conformational polymorphism, because the RMSD of the molecule overlay, entailing one of each form, only decreased significantly after the rotation of one or two torsion angles.

References	Comparison	Common molecules	Root Mean Square
UGIVAI	ENEBUW	1 out of 15	1.449
UGIVAI	ENECAD	1 out of 15	1.276
UGIVAI	UGIVAI	15 out of 15	0.000
UGIVAI01	ENEBUW	1 out of 15	0.817
UGIVAI01	ENECAD	1 out of 15	1.097
UGIVAI01	UGIVAI01	15 out of 15	0.000
UGIVAI01	UGIVAI	1 out of 15	1.017

Table D3: Crystal Packing Similarity between form I and form II and the rest of the CSD.

E. Hirshfeld Analysis

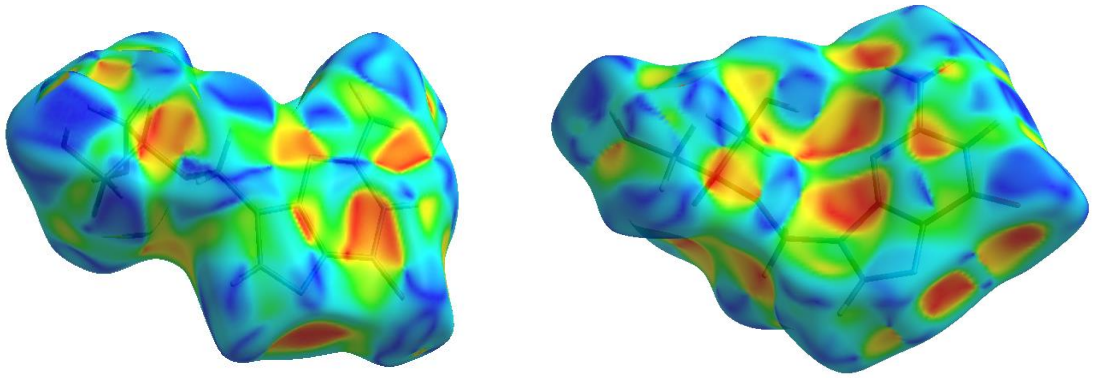

Figure E1: Shape index mapped on the Hirshfeld surface of: Left) Form I and Right) Form II. The contribution of C-H···π is shown through the relatively large indentations above the aromatic system on the shape index surface of the two forms.

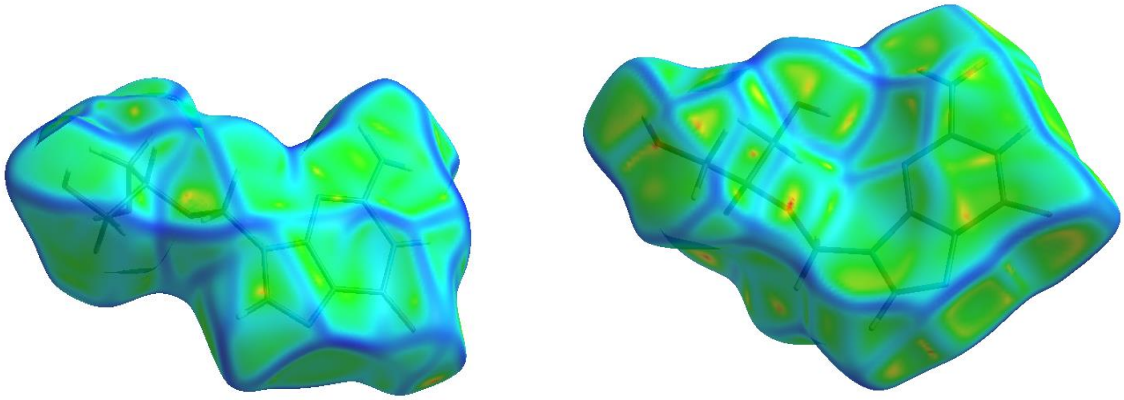

Figure E2: Curvedness Index mapped on the Hirshfeld surface of: Left) Form I and Right) Form II.

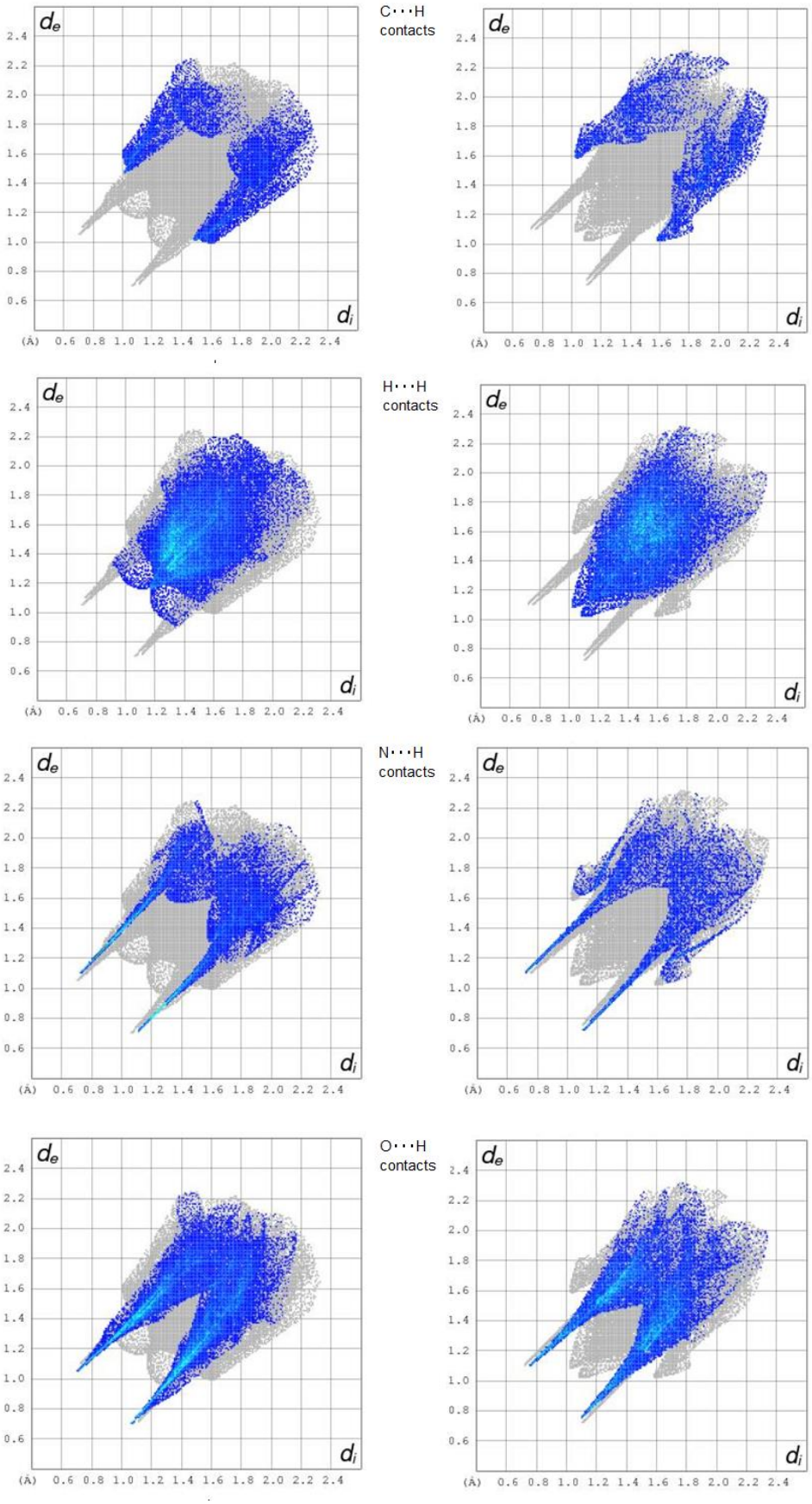

Figure E3: Fingerprint plots of first column) Form I and second column) Form II.

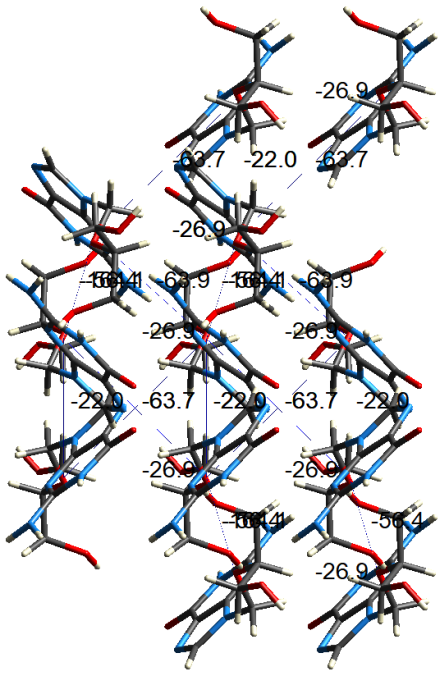

Figure E4: The energy framework of form I, showing a cluster of 3.80 Å radius, viewed along c-axis, with a cut-off of 20 kJ/mol.

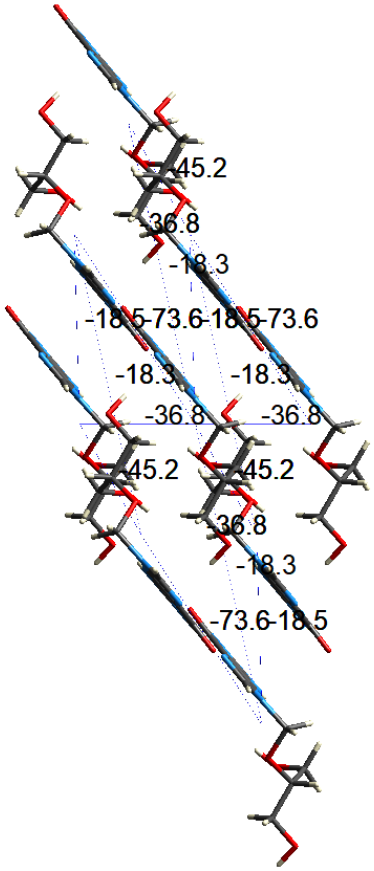

Figure E5: The energy framework of form II, showing a cluster of 3.80 Å radius, viewed along b-axis, with a cut-off of 10 kJ/mol.

F. Polymorph Assessment

The logistic regression model: $Hydrogen\ Bond\ Propensity, \phi(z) = \frac{1}{1+ e^{-z}}$

The logit function, $z = \gamma + \sum_k x_k \beta_k$

where, γ is the intercept, *x* is the predicator, β is the coefficient for each predicator and *k* is the number of predicators.[149]

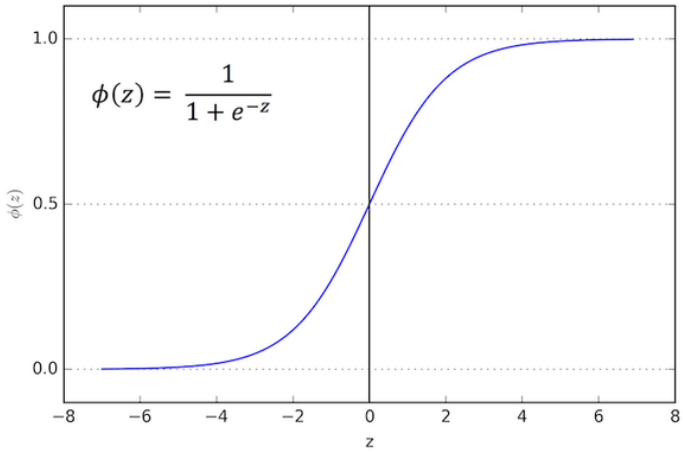

Figure F1: A curve showing the relationship between the logit function, *z* and the propensity. This can be useful during the interpretation of coefficients in relation to the hydrogen bond propensities.

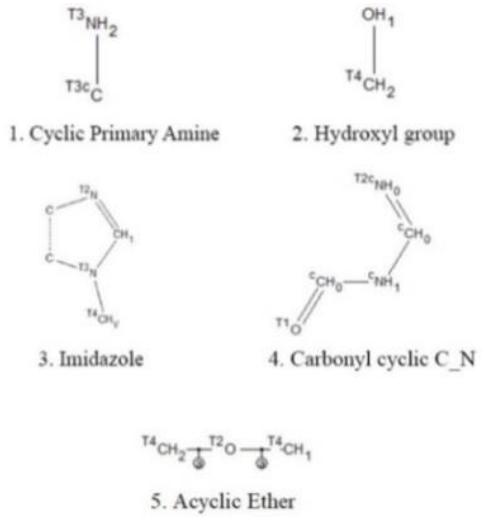

Figure F2. The substructures of ganciclovir, used for the HBP models.

	Coefficients	Estimate	Sign.	Lower bound	Upper bound
	Intercept	-0.787	***	-1.034	-0.544
Donor	Oxygen atom in hydroxyl group	0.829	***	0.629	1.032
	Nitrogen in cyclic primary amine	1.997	***	1.791	2.207
	Carbon atom in hydroxyl group	-1.028	***	-1.271	-0.786
	Nitrogen atom in carbonyl_cy C_N	0.494	***	0.275	0.716
	Carbon atom in imidazole ring	-0.186	.	-0.426	0.053
	Carbon atom bonded to imidazole ring	-0.033	.	-0.281	0.214
	Other	2.298	***	2.117	2.484
Acceptor	Nitrogen atom in cyclic primary amine	-2.654	***	-2.953	-2.371
	Nitrogen atom in imidazole ring	0.194	*	0.042	0.346
	Nitrogen atom in carbonyl_cy C_N	-0.573	***	-0.758	-0.391
	Oxygen atom in acyclic ether	-0.231	*	-0.409	-0.054
	Oxygen atom in carbonyl_cy C_N	1.012	***	0.854	1.171
	Other	1.766	***	1.656	1.876
Other	Competition	0.018	***	0.014	0.022
	Donor steric density	-0.017	***	-0.019	-0.014
	Acceptor steric density	-0.023	***	-0.026	-0.020
	Donor aromaticity	0.258	.	-0.050	0.567
	Acceptor aromaticity	0.224	.	-0.079	0.529

Table F3: The coefficients of the selected factors in the parsimonious model, together with their significance code, upper and lower bounds.

Goodness of fit data

Area under ROC curve = 0.878

Null deviance: 24735.949 on 18201 degrees of freedom

Residual deviance:15676.089 on 18183 degrees of freedom

Donor	Acceptor	Propensity	Lower bound	Upper bound
C7	N5	0.91	0.91	0.91
C6	O3	0.90	0.90	0.90
C6	O4	0.90	0.90	0.90
O3	O4	0.81	0.81	0.81
O4	O3	0.81	0.81	0.81
C6	N5	0.73	0.73	0.73
C4	O2	0.32	0.32	0.32
C8	O4	0.32	0.32	0.32
C9	O3	0.32	0.32	0.32
O3	O2	0.19	0.19	0.19
O4	O2	0.19	0.19	0.19

Table F4: The predicted intramolecular hydrogen bonding for both forms, with the atom numbering associated with form I. None of the predicted intramolecular contacts were observed by the model.

UGIVAI01

Atom (D/A)	= 0	= 1	= 2	= 3
C4 of cyclic_n (d)	0	**0**	0	0
C6 of acyclic_ether (d)	0	**0**	0	0
C9 of acyclic_al_oh (d)	0	**0**	0	0
N1 of cyclic_prim_amine (d)	0.00671913	0.112477	**0.769789**	0.111015
N2 of cyclic_amide (d)	0.0124012	**0.960872**	0.026727	0
O3 of acyclic_al_oh (d)	0.0376089	**0.905897**	0.0564941	0
O4 of acyclic_al_oh (d)	0.0435692	**0.9042**	0.0521708	0
N3 of cyclic_n (a)	0.0558296	**0.885105**	0.0590651	0
N5 of cyclic_n (a)	0.251052	**0.729221**	0.0197272	0
O1 of cyclic_amide (a)	0.0229069	0.396671	**0.550449**	0.0299725
O2 of acyclic_ether (a)	0.776348	**0.223652**	0	0
O3 of acyclic_al_oh (a)	0.216116	0.733893	**0.0499909**	0
O4 of acyclic_al_oh (a)	0.235037	**0.71847**	0.0464933	0

Table F5: Coordination table of form I.

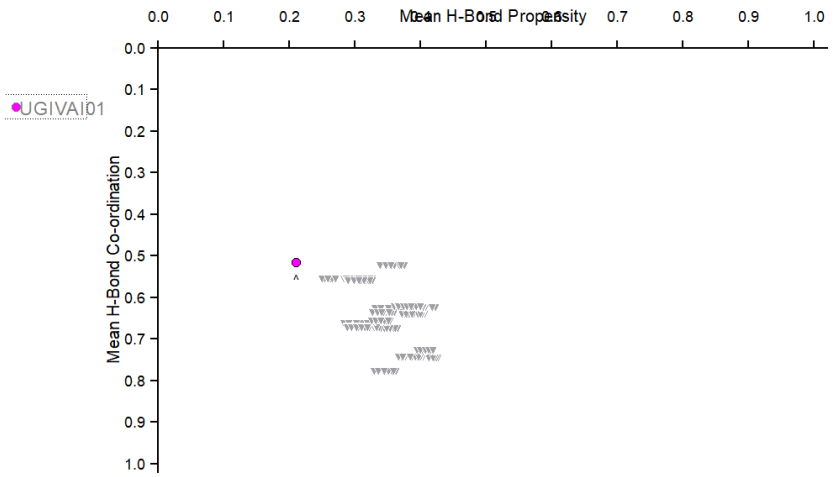

Figure F6: The propensity participation chart output for form I (violet dot).

Donor	Acceptor	Prop	Lower Bound	Upper Bound	I	II
N1 of primary amine	O1 of carbonyl_cy C_N	0.72	0.66	0.78		×
N1 of primary amine	O3 of hydroxyl group	0.52	0.45	0.58		
N1 of primary amine	O4 of hydroxyl group	0.52	0.45	0.58		×
N1 of primary amine	N3 of imidazole ring	0.49	0.42	0.56		
O3 of hydroxyl group	O1 of carbonyl_cy C_N	0.45	0.38	0.53		
O4 of hydroxyl group	O1 of carbonyl_cy C_N	0.45	0.38	0.53		×
N2 of carbonyl_cy C_N	O1 of carbonyl_cy C_N	0.35	0.29	0.41		
N1 of primary amine	O2 of acyclic ether	0.31	0.25	0.38	×	
N1 of primary amine	N5 of carbonyl_cy C_N	0.28	0.23	0.35	×	
O3 of hydroxyl group	O3 of hydroxyl group	0.26	0.22	0.31		
O3 of hydroxyl group	O4 of hydroxyl group	0.26	0.22	0.31		
O4 of hydroxyl group	O3 of hydroxyl group	0.26	0.22	0.31	×	
O4 of hydroxyl group	O4 of hydroxyl group	0.26	0.22	0.31		
O3 of hydroxyl group	N3 of imidazole ring	0.24	0.19	0.30	×	
O4 of hydroxyl group	N3 of imidazole ring	0.24	0.19	0.30		
C7 of acyclic ether	O1 of carbonyl_cy C_N	0.22	0.18	0.25		
N2 of carbonyl_cy C_N	O3 of hydroxyl group	0.18	0.15	0.23		
N2 of carbonyl_cy C_N	O4 of hydroxyl group	0.18	0.15	0.23	×	

Donor	Acceptor	Prop	Lower Bound	Upper Bound	I	II
C4 of imidazole ring	O1 of carbonyl_cy C_N	0.18	0.14	0.24	×	
C6 of imidazole ring	O1 of carbonyl_cy C_N	0.17	0.13	0.23	×	
N2 of carbonyl_cy C_N	N3 of imidazole ring	0.17	0.13	0.21		×
O3 of hydroxyl group	O2 of acyclic ether	0.13	0.10	0.17		
O4 of hydroxyl group	O2 of acyclic ether	0.13	0.10	0.17		
O3 of hydroxyl group	N5 of carbonyl_cy C_N	0.12	0.09	0.15		
O4 of hydroxyl group	N5 of carbonyl_cy C_N	0.12	0.09	0.15		
C7 of acyclic ether	O3 of hydroxyl group	0.10	0.09	0.12		
C7 of acyclic ether	O4 of hydroxyl group	0.10	0.09	0.12		
C8 of hydroxyl group	O1 of carbonyl_cy C_N	0.10	0.08	0.14		
C9 of hydroxyl group	O1 of carbonyl_cy C_N	0.10	0.08	0.14		
C7 of acyclic ether	N3 of imidazole ring	0.09	0.08	0.11		
N2 of carbonyl_cy C_N	O2 of acyclic ether	0.09	0.07	0.12		
C4 of imidazole ring	O3 of hydroxyl group	0.09	0.07	0.11		
C4 of imidazole ring	O4 of hydroxyl group	0.09	0.07	0.11		
C6 of imidazole ring	O3 of hydroxyl group	0.08	0.06	0.10		
C6 of imidazole ring	O4 of hydroxyl group	0.08	0.06	0.10		
C4 of imidazole ring	N3 of imidazole ring	0.08	0.06	0.10		
N2 of carbonyl_cy C_N	N5 of carbonyl_cy C_N	0.08	0.06	0.10		
C6 of imidazole ring	N3 of imidazole ring	0.07	0.05	0.10		
C7 of acyclic ether	O2 of acyclic ether	0.05	0.04	0.06		
C8 of hydroxyl group	O3 of hydroxyl group	0.04	0.03	0.06		
C8 of hydroxyl group	O4 of hydroxyl group	0.04	0.03	0.06		
C9 of hydroxyl group	O3 of hydroxyl group	0.04	0.03	0.06	×	
C9 of hydroxyl group	O4 of hydroxyl group	0.04	0.03	0.06		
C7 of acyclic ether	N5 of carbonyl_cy C_N	0.04	0.03	0.05		
C8 of hydroxyl group	N3 of imidazole ring	0.04	0.03	0.05		
C9 of hydroxyl group	N3 of imidazole ring	0.04	0.03	0.05		
C4 of imidazole ring	O2 of acyclic ether	0.04	0.03	0.05		
C6 of imidazole ring	O2 of acyclic ether	0.04	0.03	0.05		
C4 of imidazole ring	N5 of carbonyl_cy C_N	0.03	0.02	0.05		

C6 of imidazole ring	N5 of carbonyl_cy C_N	0.03	0.02	0.04		
C8 of hydroxyl group	O2 of acyclic ether	0.02	0.01	0.03		
C9 of hydroxyl group	O2 of acyclic ether	0.02	0.01	0.03		
C8 of hydroxyl group	N5 of carbonyl_cy C_N	0.02	0.01	0.02		
C9 of hydroxyl group	N5 of carbonyl_cy C_N	0.02	0.01	0.02		

Table F7: The list of predicted intermolecular hydrogen bonds.

The interactions with the highest propensities belonged to form II, with the maximum one involving the nitrogen atom of the amine group and the carbonyl oxygen. The strong potential of both respective participants was detected by the peaks of the electrostatic map and the intense full interaction maps surrounding both locations. Despite of the high potential of nitrogen in the amine group to act as a donor, the observed contacts in form I, involving such nitrogen were still of much lower probability, because they incorporated an ether oxygen and an aromatic nitrogen as acceptors. Due to the presence of very competitive functional groups, it was expected that any contact involving a carbon donor would have very small probability.